Estimation of Surface Heat Fluxes around Kherlen River Basin by Airborne Turbulence Data

KOTANI Ayumi and SUGITA Michiaki
Graduate School of Life and Environmental Sciences, University of Tsukuba, Japan

Key words: convective boundary layer, variance methods, aircraft observation

1.Introduction

The aircraft observation has an advantage in deriving area-averaged values and detecting the spatial variability, although it requires careful instrument settings and data processing especially in case of using wind data in eddy correlation method to evaluate fluxes (e.g., Lenschow, 1986). The variance methods to estimate surface fluxes from the associated variances measurements in the surface or mixed layer on the other hand are appealing in this context because it is possible to derive surface fluxes without observing wind velocity. The variance methods have been applied to surface layer and produced satisfied results (e.g., Wesely, 1988). On the contrary, convective boundary layer (CBL), where the flux-variance relationship is not fully understood and established yet. Until now, only a limited number of studies are available on this topic with examples of Asanuma (1996) from aircraft and Sugita and Kawakubo (2003) from tower observation of the lower half of the convective boundary layer.

The purpose of this study is to investigate validityof CBL variance methods and to improve them.

2. Methods

Aircraft observation

The temperature turbulence data were obtained by aircraft observation carried out from June to October of 2003 as a part of the field observation of RAISE (Rangelands Atmosphere-Hydrosphere-Biosphere Interaction Study Experiment in Northeastern Asia). The RAISE study area covers the Kherlen river basin, the arid to semi-arid region in northeastern Mongolia, with a boreal forest in northern and upper watershed and grassland (Steppe) area towards the southern and downstream part. The instruments were installed to a wing of an aircraft, AN2 to measure scalar variables of the air temperature and humidity with a fine thermocouple (CC-type) and a Kripton hygrometer (KH20, Campbel Scientific Inc.). The data were sampled at 10Hz. Also positioning information was obtained by a GPS receiver. The flight path covered the experimental area (Figure 1) and several heights of 100, 200, 500 and 1000m were flown repeatedly above the ground observation site (see below). Although each path length is different depending on the weather condition, those with flight paths longer than 5 km, which is equivalent to 100 s of averaging time, and with the standard deviation of the flight level within 30 m have been selected for analysis. For each path, the data have been processed to remove a trend by a linear regression method before the analysis.

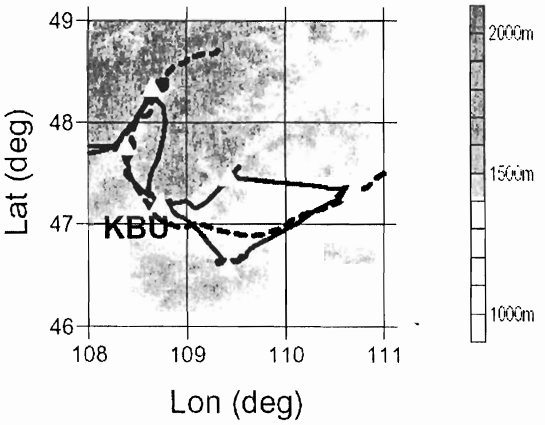

Figure 1. Study area. solid line: flight path (8/23,24), broken line: Kherlen river, triangle: ground based observation site. KBU flux station is the main study area of this analysis.

Ground based observation

Within the grassland area, one flux station and four automatic weather stations (AWSs) were in operation during the flights. At the flux stations, the surface fluxes of sensible heat and water vapor were directly measured by the eddy correlation method every 30 minutes (Kojima, 2004). Since the eddy correlation flux data showed the energy imbalance, the energy shortage has been distributed into the turbulence energy flux by keeping Bowen ratio (Twine et al., 2000) for this analysis. During the flight time, average closed ratio (ratio of turbulence energy measured by eddy correlation methods to available energy) was 0.67, and corrected sensible heat flux ranged from 80 to 200 Wm-

2. Meteorological data

The output of regional climate model (TERC-RAMS, Kimura and Sato, 2005), which was downscaled from 6-hourly NCEP/ NCAR reanalysis (Kalney et al., 1996), was used to evaluate mesoscale or synoptic scale atmosphere conditions. This dataset has resolution of 30 km in horizontal and one hour in time.

3. Results

In the convective boundary layer (CBL), turbulence statistics were found to follow the convective (or mixed-layer) scaling. The aircraft observed temperature variance *óè* is scaled with temperature scale

$$T_* = \left[\theta\left(\overline{w\theta_0}\right)^2 (gh_i)^{-1}\right]^{1/3} \qquad (1)$$

where *è* is potential temperature and 0 ' ' è *w* is surface temperature flux, and *hi* is boundary layer height. The dimensionless *óè T** -1 are plotted against *î* = *zhi* -1, where *z* is sensor height in Figure 2 with some formulation proposed in previous studies (see below). The boundary layer height *hi* was estimated by the method proposed by Liu and Ohtaki (1997) with spectral data of horizontal velocity observed at the flux stations (KBU).

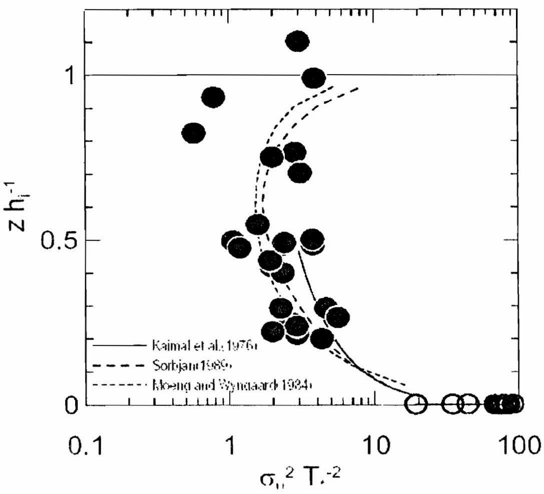

Figure 2. Vertical profile of normalized variance of Θ observed at grassland area (KBU). open circle: ground based measurements, closed circle: aircraft measurements. Three functional line present the formulation (2), (5) and (6). óè T*

The height of CBL is around 700 – 1200 m. The observed values follow the functional forms in general except for the upper part of CBL, where the scatter is relatively larger probably because of the entrainment flux dominating near the inversion layer.

Kaimal et al. (1976) obtained with observation data for $0.1 < zh_i^{-1} < 0.5$

$$\frac{\sigma_\theta^2}{T_*^2} \approx 1.8\xi^{-2/3} \qquad (2)$$

Others have included the whole boundary layer diffusion process with the top-down and bottom-up (TDBU) model (Moeng and Wyngaard, 1984), which separates the source of the boundary layer diffusion process into the surface and the inversion origins, and can be written in general form by Asanuma (1996),

$$\sigma_\theta^2 = \left(\frac{\overline{w'\theta'_h}}{v_h}\right)^2 f_t(\xi) - 2\left(\frac{\overline{w'\theta'_h}\,\overline{w'\theta'_0}}{v_h\,v_0}\right) f_{tb}(\xi) - \left(\frac{\overline{w'\theta'_0}}{v_0}\right)^2 f_b(\xi) \qquad (3)$$

where *vh* and *v0* are the velocity scale at the inversion base and at the surface, respectively. These scales should include the effect of surface shear and the convective (buoyant) forcing. Therefore available selection can be the friction velocity *u**, convective velocity *w** and their combination, for example. In this study, *w** is used for both *vh* and *v0* as Moeng and Wyngaard (1984) did. The symbol *ft*, *ftb* and *fb* are universal functions of *î*. Assuming that the inversion flux is proportional to surface flux, study, *w** is used for both *vh* and *v0* as Moeng and Wyngaard (1984) did. The symbol *ft*, *ftb* and *fb* are universal functions of *î*. Assuming that the inversion flux is proportional to surface flux,

$$\overline{w'\theta'_h} = -A_\theta\overline{w'\theta'_0} \qquad (4)$$

where *Aè* is entrainment constant for sensible heat flux, typically 0.2 – 0.3 (e.g., Stull, 1976). With those assumption, (3) can be rewritten to

$$\frac{\sigma_\theta^2}{T_*} = A^2 f_t(\xi) - 2A f_{tb}(\xi) + f_b(\xi) \qquad (5)$$

A similar functional form was proposed by Sorbjan (1989), which decompose statistical variables to a non-penetrative part and a residual part.

$$\frac{\sigma_\theta^2}{T_*^2} = C_{M\theta 0} \frac{(1-z/h)^{4/3}}{(z/h)^{2/3}} + C_{M\theta i} A_\theta^{4/3} \frac{(z/h)^{4/3}}{(1-z/h-D)^{2/3}} \qquad (6)$$

where D=h_j^{-1} with the depth of the interfacial layer on the top of the mixed layer ., *CMè0* and *CMèi* are the constants, which depend on the value of *Aè* .

These functions are also shown in Figure 2. The deviation of observed values from those existing formulations could be caused by the inadequate experimental constants included in those equations. From the viewpoint of flux estimation, (2), (5) and (6) were rewritten to obtain surface flux 0 ‘ ‘ è *w* by following Sugita and Kawakubo (2003). As mentioned, the constants in those equations are still not well established and further studies are needed. As such, in the present analysis, first those constants previously proposed were applied and then they were calibrated with the current data sets. The calibration was performed in the same manner as Sugita and Kawakubo (2003), where a part of coefficients were changed at a small step until the root mean square (rms) difference between the estimated flux and reference flux became the smallest. These results are shown on Figure 3 to 5 and Table 1, where the rms differences are about 40 Wm-2 after the calibration of the constants as will be mentioned later.

The scatter that still exists could be explained with the relevant parameters other than *z*, *hi* and 0 ‘ ‘ è *w* . The possible variables include the Coriolis parameter *f*, the Ekman layer depth *hr* = *ê u* f*-1(*ê*: constant, *u**: friction velocity), the Obkhov length *L*. Furthermore, the vertical gradient of geostrophic wind (i.e., baloclinity) .*Ug*/.*z*, .*Vg*/.*z*. and horizontal gradient of advection .(*uè*)/.*x*,

.(*vè*)/.*y*. These were evaluated with the output of the

regional climate model as described before. *Ug* and *Vg*

are northward and eastward components of the geostrophic wind and they are given by the gradient of altitude on 750 hPa isobaric surface.

ith these variables, the variance equations (2), (5) and (6) could be rewritten, based on the similarity argument. The number of dimension is three (length, time and temperature), thus with these eight relevant parameters, five dimensionless parameters could be created by partly following Brutsaert and Mawdsley (1976), who discussed the variables effective to the mean profiles of the whole ABL,

$$\xi = z / h_i \qquad (7)$$

$$\mu_i = h_i / L \qquad (8)$$

$$\nu_0 = h_i / h_r \qquad (9)$$

$$\gamma = \left\{ \left(\frac{\partial \overline{u\theta}}{\partial x} \frac{h_i}{\overline{w\theta_0}} \right)^2 + \left(\frac{\partial \overline{v\theta}}{\partial y} \frac{h_i}{\overline{w\theta_0}} \right)^2 \right\}^{1/2} \qquad (10)$$

$$\beta = \left[\left\{ \frac{\partial u_g}{\partial z} \left(\frac{h_i}{h_i} \right)^2 \frac{1}{|f|} \right\}^2 + \left\{ \frac{\partial v_g}{\partial z} \left(\frac{h_i}{h_i} \right)^2 \frac{1}{|f|} \right\}^2 \right]^{1/2} \qquad (11)$$

Note that ã and â include two horizontal components, which are treated separately in previous study, where direction of *u* and *v* presents that of surface shear stress and normal to it.

Among those dimensionless variables, î had already been included in the variance profile formulation (2), (5) and (6). Therefore other four were added in the following equations,

$$\left(\frac{\sigma_\theta}{T_*} \right)^2 = F(z / h_i) + a_1 \mu_i^{a_2} + a_3 \nu_0^{a_4} + a_5 \beta^{a_6} + a_7 \gamma^{a_8} + a_9 \qquad (12)$$

where *F* is function of *î*, which corresponds to the right hand side of (2), (5) and (6). This equation can be solved for 0 ‘ ‘ *w* (inside *T**), and the coefficients *a1 – a9* are determined to minimize the rms difference between the estimated and observed values. To investigate which parameter has more contribution to the estimation of fluxes, all combination of parameters were tested. The rms difference decreased as the number of parameters increased. However there is no specific parameter that has a larger influence to reduce the rms error.

Lastly, the results of calibrated constants and addition of parameters to the function are shown in Figure 3 to 5 and Table 1. The rms differences reduced to about 40 Wm-2 after the calibration of the constants and about 30 Wm-2 with the additional dimensionless parameters. The former results are comparable to the result obtained with tower based measurements by Sugita and Kawakubo (2003). A little better result was given by formulation (5) and (6) than (2), probably because (2) is for lower half of boundary layer while (5) and (6) are applied to the whole layer. Though scattering of data seems large at upper layer by the entrainment from the free atmosphere, expression of entrainment flux effects in (5) and (6) are valid in this case.

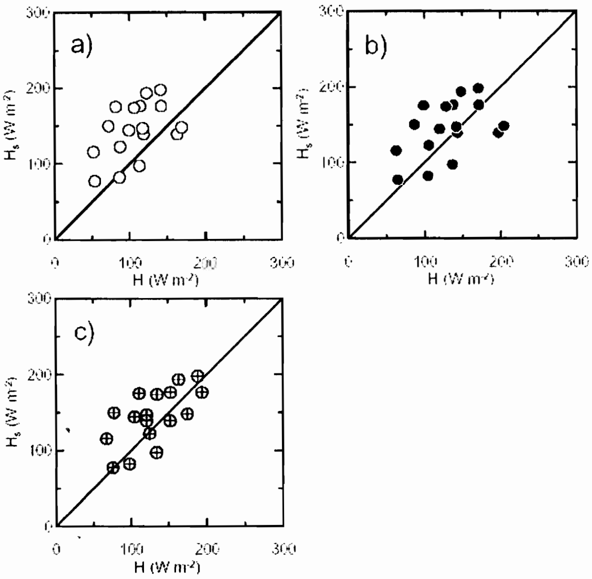

Figure 3. Comparison between the sensible heat flux *H* estimated with variance methods based on formulation (2) and *Hs* observed at ground by eddy correlation methods (KBU flux site). (a) original formulation, (b) original formulation with calibrated constants, (c) formulation of (b) added dimensionless parameters.

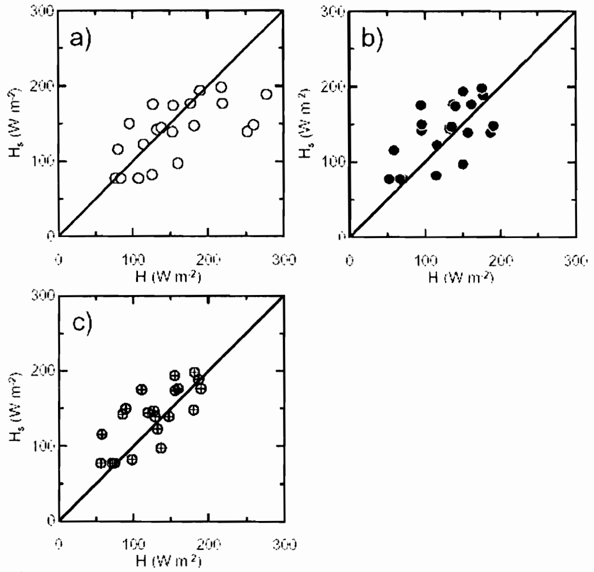

Figure 4. same as Figure 3 but for variance formulation (5)

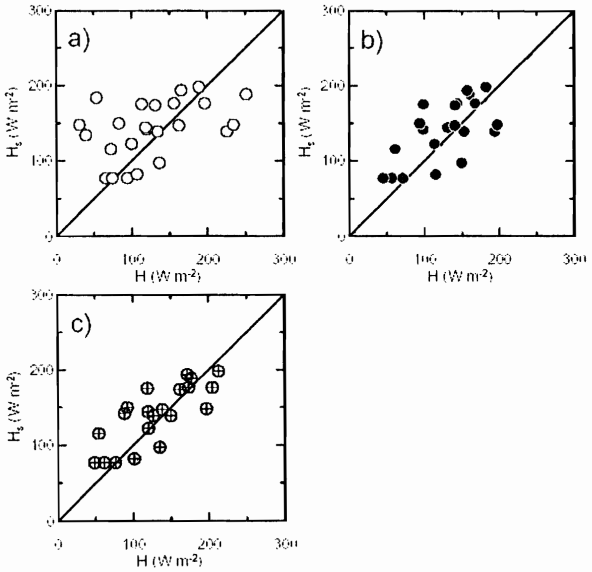

Figure 5. same as Figure 3 but for variance formulation (6)

Table 1. Result of variance methods

Equation	Number of data	rms difference (Wm^{-2})*
(2)	17	50.3 • •41.0 • •31.9
(5)	21	49.0 • •37.3 • •28.4
(6)	21	42.0 • •37.7 • •31.3

* original constant • • calibrated constant • • calibrated constant, added parameters

4. Conclusions

Turbulence data obtained by aircraft observations in CBL were analyzed to estimate the surface fluxes by means of variance methods. Observed temperature variances followed in general the CBL scaling and produced the surface heat fluxes with about 50Wm-2 of rms difference against ground based eddy correlation fluxes. The calibration of the experimentally determined coefficients within the equations reduced the difference to 40Wm-2. Furthermore, additional parameters, which represent the large scale atmospheric conditions such as baloclinity or advection, the difference were reduced to about 30 Wm-2. This rather large error relative to reference value is partly due to uncertainty of other parameters such as CBL height.

References

Asanuma, J. (1996): Turbulence Variance Characteristics in the Unstable Atmospheric Boundary Layer above Flat Pine Forest, Ph.D. Thesis, Cornell University, 118 p.

Brutsaert, W. and Mawley, J. A. (1976): The applicability of planetary boundary layer theory to calculate regional evapotranspiration. *Water Resour. Res.*, 12, 852-858.

Kaimal, J. C., Wyngaard, J. C., Haugan, D. A., Cote, O. R. and Izumi, Y. (1976): Turbulence Structure in the Convective Boundary Layer. *J. Atmos. Sci.*, 33, 637-662.

Kalney, E. and coauthors (1996): The NCEP/ NCAR 40-year reanalysis project, *Bull. Amer. Meteor. Soc.*, *74*, 789-799.

Kimura, F. and Sato, T. (2005): Downscaling of precipitation over Mongolia using regional climate model. *Bull. Terrestrial Environ. Res. Center, Univ. Tsukuba*, 5, Suppl., 110-111.

Kojima, T. (2004): The investigation of the factors which govern evapotranspirarion of Kherlen river basin in Mongolia. MSc Thesis, University of Tsukuba,85p.

Lenschow, D.H. (1986): Aircraft Measurements in the Planetary Boundary Layer. In *Probing the Atmospheric Boundary Layer*, 5-18 pp. Am. Meteorol. Soc., Boston. Liu, X., and Ohtaki, E. (1997): An Independent Method to Determine the Height of the Mixed Layer, *Boundary-Layer Meteorol.*,85, 497-504.

Moeng, C.-H. and Wyngaard, J.C. (1984): A Comparison of Shear- and Buoyancy-Driven Planetary Boundary Layer Flow. *J. Atmos. Sci*., 41, 3161-3169.

Sorbjan, Z. (1989): Structure of the Atmospheric Boundary Layer, Prentice Hall, New Jersey, 317 p.

Stull, R. B. (1976): The energetics of entrainment across a density interface. *J. Atmos. Sci.*, 33, 1260 – 1267.

Sugita, M. and N. Kawakubo (2003): Surface and Mixed-layer Variance Methods to Estimate Regional Sensible Heat Flux at the Surface. *Boundary-Layer*

Meteorol.,106,117-145. Twine, T.E., Kustas, W. P., Norman, J. M., Cook, D. R., Houser, P. R., Meyers, T. P., Prueger,, J. H., Starks, P.

J. and Wesely, M. L.(2000): Correcting eddy-covariance flux underestimates over a grassland. *Agric. For. Meteorol.*, 103, 279-300.

Wesely, M. (1988): Use of Variance Techniques to Measure Dry Air-surface Exchange Rates. *J. Atmos. Sci.*, 44, 13-31.